

Structure of $\text{CaO-Ga}_2\text{O}_3\text{-GeO}_2$ glasses: X-ray and molecular dynamics simulation studies

BOHDAN PADLYAK*

Institute of Experimental Physics, University of Gdańsk, ul. Wita Stwosza 57, 80-952 Gdańsk, Poland.

STEPAN MUDRY, VOLODYMYR HALCHAK, ANDRIJ KOROLYSHYN

Department of Physics, Ivan Franko National University of Lviv, Dragomanov Str. 50, 79-005 Lviv, Ukraine.

JAROSŁAW RYBICKI, AGNIESZKA WITKOWSKA

Faculty of Technical Physics and Applied Mathematics, Technical University of Gdańsk, ul. Narutowicza 11/12, 80-952 Gdańsk, Poland.

The X-ray scattering data for $\text{CaO-Ga}_2\text{O}_3\text{-GeO}_2$ glasses of stoichiometric compositions similar to that of calcium-gallium-germanium garnet ($\text{Ca}_3\text{Ga}_2\text{Ge}_3\text{O}_{12}$), Ca-gallogermanate ($\text{Ca}_3\text{Ga}_2\text{Ge}_4\text{O}_{14}$), and $\text{Ca}_3\text{Ga}_2\text{O}_6$ crystals are presented. Experimental results show true glass structure of the compounds under investigation. A comparative analysis of the X-ray data for glasses and their crystalline analogies has shown that the glass network consists of gallium and germanium oxygen co-ordinated octahedra and tetrahedra. The results obtained have been compared with the results of preliminary molecular dynamics (MD) calculations of the structure of $\text{CaO-Ga}_2\text{O}_3\text{-GeO}_2$ glasses. The pair distribution functions (PDFs), obtained from the MD simulation, show satisfactory agreement with the X-ray data. The building blocks of the $\text{CaO-Ga}_2\text{O}_3\text{-GeO}_2$ glass network have been proposed. The structure peculiarities of the glasses and their crystalline analogies are discussed.

1. Introduction

Disordered crystals and glass matrices doped with transition and rare earth metal ions are still attractive as a possible laser medium, especially for tunable solid state lasers. This also refers to the low-field Cr^{3+} ions in disordered crystals and glasses owing to the homogeneous, as well as inhomogeneous broadening of the optical transitions. Up to date, the structure and peculiarities of the ligand field for activator ions in disordered crystals and glasses have been studied insufficiently, because correct interpretation of spectroscopic data requires detailed information on real structure of disordered crystals and glasses. Structural investigations of complex disordered crystals and glasses are connected with difficulties of X-ray experimental

* On leave in the Department of Physics, Ivan Franko National University of Lviv, Dragomanov Str. 50, 79-005 Lviv, Ukraine.

data analysis. Therefore, compounds which can be obtained in both crystalline and vitreous (or glassy) phases are ideal objects for structural studies.

For our investigation we have chosen $\text{CaO-Ga}_2\text{O}_3\text{-GeO}_2$ and $\text{CaO-Ga}_2\text{O}_3$ systems. In the ternary $\text{CaO-Ga}_2\text{O}_3\text{-GeO}_2$ system, three stable crystalline forms exist: $\text{Ca}_3\text{Ga}_2\text{Ge}_3\text{O}_{12}$ (ordered garnet structure – $Ia3d$ space group), $\text{Ca}_3\text{Ga}_2\text{Ge}_4\text{O}_{14}$ (substitutionally or compositionally disorderd Ca-gallogermanate structure – $P321$ space group), $\text{Ca}_2\text{Ga}_2\text{GeO}_7$ (gelenite structure – $P4_21m$ space group) [1], [2] In the binary $\text{CaO-Ga}_2\text{O}_3$ system also three stable crystalline compounds exist: $\text{Ca}_3\text{Ga}_2\text{O}_6$, $\text{Ca}_2\text{Ga}_2\text{O}_5$, CaGa_2O_4 [2]. The glasses with $\text{Ca}_3\text{Ga}_2\text{Ge}_3\text{O}_{12}$, $\text{Ca}_3\text{Ga}_2\text{Ge}_4\text{O}_{14}$ and $\text{Ca}_3\text{Ga}_2\text{O}_6$ stoichiometric compositions were prepared as described in [3].

Preliminary results of structural investigation of $\text{CaO-Ga}_2\text{O}_3\text{-GeO}_2$ glasses by X-ray diffraction technique were described in [4], [5]. The present paper aims at a much more detailed X-ray study of the structure of undoped $\text{Ca}_3\text{Ga}_2\text{Ge}_3\text{O}_{12}$, $\text{Ca}_3\text{Ga}_2\text{Ge}_4\text{O}_{14}$ and $\text{Ca}_4\text{Ga}_2\text{O}_6$ glasses, and comparison of the results with structural data for corresponding crystals. Moreover, the X-ray diffraction data for glassy phase are compared with the results of preliminary MD simulations.

2. Experimental details

The $\text{CaO-Ga}_2\text{O}_3\text{-GeO}_2$ glasses of high chemical purity and optical quality, with various stoichiometric compositions, both undoped and doped with transition metal ions, were prepared in corundum crucibles by standard high-temperature synthesis [3]. The chemical composition of the glasses obtained was controlled by X-ray microanalysis method, using a Camebax apparatus. The undoped glasses with stoichiometric compositions similar to that of $\text{Ca}_3\text{Ga}_2\text{Ge}_3\text{O}_{12}$, $\text{Ca}_3\text{Ga}_2\text{Ge}_4\text{O}_{14}$ and $\text{Ca}_3\text{Ga}_2\text{O}_6$ crystals were submitted to structural studies.

In order to obtain information on atomic arrangement in $\text{CaO-Ga}_2\text{O}_3\text{-GeO}_2$ glasses, the X-ray scattering method was used. The experimental data were obtained as a dependence of X-ray scattered intensity versus the scattering angle. For this purpose we used a special chamber attached to the X-ray diffractometer, which allowed investigation of the structure, both in vacuum and in inert atmosphere. The $\text{Cu } K_\alpha$ -radiation, monochromatised by LiF crystal, was scattered by the sample and recorded by an NaJ:Tl detector. The scattering angle was being changed within the range from 10° up to 140° and measured with the accuracy of $\pm 6''$. The counting time of impulses was long enough, so that the error in the measured intensity did not exceed 3%. Experimental values of the scattered intensity were corrected for polarisation, absorption, and incoherent scattering, and then used for evaluation of the structural factor (SF), as described in [6].

3. Simulation technique

Molecular dynamics simulations have been performed in the microcanonical (NVE) ensemble. The atoms were assumed to interact by a two-body potential

(Born–Mayer repulsive forces, and Coulomb forces, calculated with the aid of the standard Ewald technique). The Ge–Ge, Ge–O, and O–O interaction parameters were taken from [7] and for Ca–Ca, Ga–Ga pairs the data from [8] were used. The Ca–Ga, Ca/Ga–O and Ca/Ga–Ge cross-interaction parameters were calculated as suitable averages of the Ca–Ca, Ga–Ga, Ge–Ge and O–O interactions using the Lorenz–Berthelot mixing rule. Full ionic charges Ca^{2+} , Ga^{3+} , Ge^{4+} , and O^{2-} were used. All the samples were prepared initially as well equilibrated melts at the temperature of 6000 K. Then they were slowly cooled down to 300 K, passing intermediate temperatures of 5000, 4000, 3000, 2500, 2000, 1500, 1000 and 600 K. At each temperature the systems were being equilibrated during 8000 fs time steps, and sampled during other 2000 time steps.

4. Results and discussion

The structural investigations by X-ray diffraction technique show that the obtained $\text{CaO-Ga}_2\text{O}_3\text{-GeO}_2$ compounds have a true glass structure. The measurement results for glasses of various stoichiometric compositions are presented in Figs. 1 – 4.

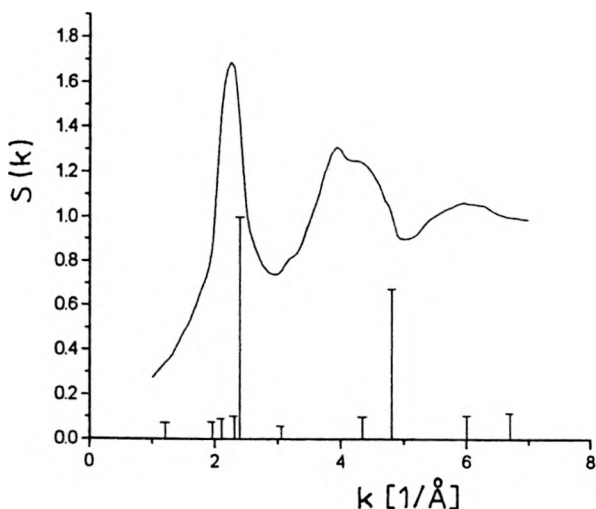


Fig. 1. Structure factor for crystal and glass of $\text{Ca}_3\text{Ga}_2\text{O}_6$ composition.

4.1. Structure factors

Figures 1 – 3 show SFs for the compounds in crystalline and glassy states. The X-ray structural data for crystalline $\text{Ca}_3\text{Ga}_2\text{Ge}_3\text{O}_{12}$, $\text{Ca}_3\text{Ga}_2\text{Ge}_4\text{O}_{14}$ and $\text{Ca}_3\text{Ga}_2\text{O}_6$ were taken from [1], [2]. As can be seen, there are significant differences between the SFs.

For $\text{Ca}_3\text{Ga}_2\text{O}_6$ glasses (Fig. 1), the profile of SF is characterized by three peaks. The first of them is expanded on the left-hand side of the principal peak, which for more massive samples transforms into a pre-peak at about $k = 1.2 \text{ \AA}^{-1}$. The ratio of the first and the second maximum heights is typical of most glasses and amorphous

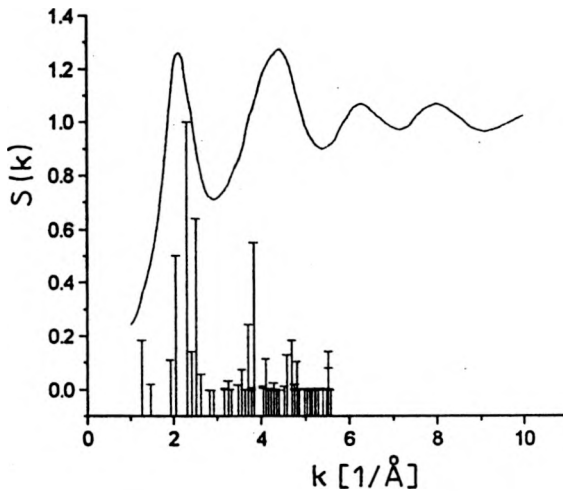


Fig. 2. Structure factor for crystal and glass of $\text{Ca}_3\text{Ga}_2\text{Ge}_3\text{O}_{12}$ composition.

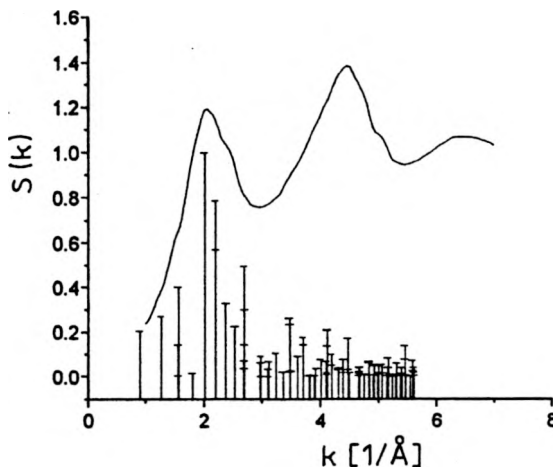


Fig. 3. Structure factor for crystal and glass of $\text{Ca}_3\text{Ga}_2\text{Ge}_4\text{O}_{14}$ composition.

alloys. It should be noted that the SF for $\text{CaO-Ga}_2\text{O}_3\text{-GeO}_2$ glasses significantly depends on the preparation technology parameters. The SFs for larger samples show the existence of a crystalline phase, too. Vertical bars in Fig. 1 indicate the X-ray pattern from the crystalline phase. It is clear that correlation between the first maximum position of the SF and of the X-ray pattern of crystalline phase is fairly good, whereas for the second peak is rather poor. This fact allows us to conclude that the short-range ordering in glasses and crystals is similar, but atomic correlations within the further co-ordination shells of glass network are more complicated than in the crystal lattice.

For the $\text{Ca}_3\text{Ga}_2\text{Ge}_3\text{O}_{12}$ glass, the SFs (Fig. 2) have profiles essentially different from those for the $\text{Ca}_3\text{Ga}_2\text{O}_6$ glass discussed above, in which the Ge atoms were

absent. The principal peak height is lower, and its position is shifted towards smaller k -values. The left-hand side of the first peak shows a good resolution and has no pre-peak (Fig. 2). The second maximum occupies almost the same position but the third one splits into two sub-peaks. The comparison with crystalline X-ray pattern shows a sufficiently good correlation in the region of the first peak, and somewhat worse for the second maximum (Fig. 2). Nevertheless, the two intensive peaks for crystalline phase are not observed in the structure factor for the glass. Thus, we can state that although the crystal-like atomic arrangements do appear in vitreous state, a certain part of atoms is rearranged in respect of the corresponding crystal.

The SF for vitreous $\text{Ca}_3\text{Ga}_2\text{Ge}_4\text{O}_{14}$ also agrees with crystalline pattern in the range of the first peak (Fig. 3). The most intensive maxima are located in the region of the first peak profile, reproduced the X-ray pattern for glass. The height of the first maximum is lower than the height of the second one. A large width of the first peak is related to a wide distribution of positions of the crystalline maxima. The second maximum also shows such a correlation, although certain discrepancies are observed (Fig. 3).

Taking into account these experimental data we can state that the chemical ordering, characteristic of crystalline phases, exists also in glasses. The specific crystalline structure of each chemical compound is revealed in the SFs of the corresponding glasses and, consequently, we can suppose that chemical short-range interactions are the dominant factor in formation of the glassy structure. The addition of Ge atoms to vitreous $\text{Ca}_3\text{Ga}_2\text{O}_6$ significantly changes its structure. Adding them to vitreous $\text{Ca}_3\text{Ga}_2\text{Ge}_3\text{O}_{12}$ modifies the structure less distinctly (substitutions for the Ga atoms). Although Ge-atoms often attempt to form amorphous Ge-like structures, this is not the case here. That can be connected with lack of Ge, because GeO_2 is the most volatile component of the melt.

4.2. Radial distribution functions

Figure 4 presents pair distribution functions calculated as Fourier transforms of the experimental structure factors. These functions show two sharp maxima only. The other maxima are smeared out, which indicates that the atomic ordering is not significant at larger distances.

For vitreous $\text{Ca}_3\text{Ga}_2\text{O}_6$ the first peak has its maximum at $r = 2.05 \text{ \AA}$ (Fig. 4, curve 1). Taking the value of k_1 from the proper SF we obtain $(r_1 k_1) = 4.4$, which according to the classification given in [9] allows us to consider this peak as a precursor of chemical short range ordering. The first peak in the $g(r)$ most probably corresponds to Ca-O and Ga-O correlations. The second peak, located at $r = 3.5 \text{ \AA}$ describes the correlation between Ca and Ga, *i.e.*, Ca-Ca, Ga-Ga, and Ca-Ga correlations. Due to such correlations this maximum is wider than the first one.

When a sufficient amount of GeO_2 is added to $\text{CaO-Ga}_2\text{O}_3$ system, a glass of composition $\text{Ca}_3\text{Ga}_2\text{Ge}_3\text{O}_{12}$ can be produced. Its structure is somewhat different from the structure of $\text{Ca}_3\text{Ga}_2\text{O}_6$. The $g(r)$ first maximum is higher and more resolved

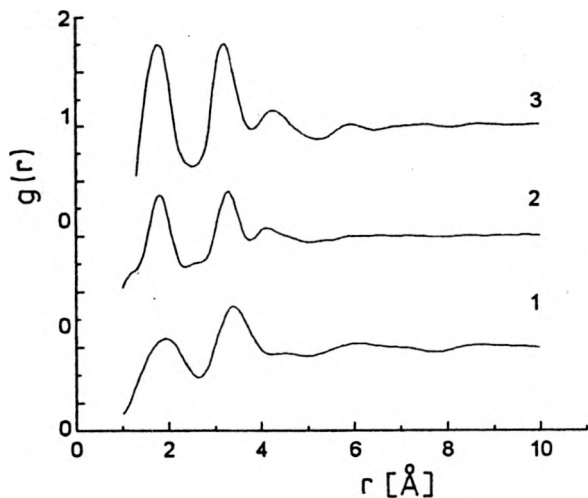


Fig. 4. Pair distribution functions for glasses of $\text{Ca}_3\text{Ga}_2\text{O}_6$ (1), $\text{Ca}_3\text{Ga}_2\text{Ge}_3\text{O}_{12}$ (2), and $\text{Ca}_3\text{Ga}_2\text{Ge}_4\text{O}_{14}$ compositions.

(*cf.* curves 1 and 2 in Fig. 4). The same refers to the maxima in the corresponding SF (Figs. 1 and 2). The hump between the first and the second maxima is pronounced. The $(k_1 r_1)$ value in this case is equal to 3.8, which also confirms the appearance of chemical ordering. The value of $(k_1 r_1)$ lower than that in vitreous $\text{Ca}_3\text{Ga}_2\text{O}_6$ indicates more pronounced chemical ordering. We assume the first peak of $g(r)$ to be the sum of three peaks, corresponding to the Ca–O, Ga–O and Ge–O correlations. The second maximum at $r = 3.30 \text{ \AA}$ is the sum of the Ca–Ga, Ca–Ge and Ga–Ge correlations. It is clear that the above correlations contribute to the total peak in different ways.

For the next vitreous compound, $\text{Ca}_3\text{Ga}_2\text{Ge}_4\text{O}_{14}$, the pair correlation is similar as in the previous case, but the first peak is more resolved (*cf.* curves 2 and 3 in Fig. 4). The value of $(k_1 r_1)$ is equal to 3.6, and is similar as in vitreous $\text{Ca}_3\text{Ga}_2\text{Ge}_3\text{O}_{12}$. The first maximum position is slightly shifted to smaller k -values. This peak is again responsible for the Ca–O, Ga–O, and Ge–O correlations, but contribution of the latter is smaller than in the previously considered compounds.

4.3. Most probable inter-atomic distances

Let us compare the most probable inter-atomic distances (obtained from pair distribution functions as the peak maxima positions) with those for the corresponding crystalline compounds. In crystalline $\text{Ca}_3\text{Ga}_2\text{Ge}_3\text{O}_{12}$, the Ca–O distances amount approximately to 2.39 \AA and 2.53 \AA , being significantly larger than in the corresponding glass (1.80 \AA). The Ga–O distance equals 2.09 \AA , and falls onto the right-hand side wing of the first $g(r)$ peak for the glasses. The Ge–O crystalline inter-atomic distance (1.65 \AA) reveals a better agreement with the Ge–O distance in the glass. The former falls onto the left-hand side of the first peak for the glass. Thus, upon transition to the vitreous state, some distances in crystalline phase become

shorter (Ca–O, Ga–O) and other longer (Ge–O). The second maximum of glass $g(r)$ function (3.3 Å) is the closest to crystalline inter-atomic distances Ge–Ca (3.06 Å), Ca–Ca (3.75 Å), Ca–Ga, Ga–Ge (3.42 Å).

In crystalline $\text{Ca}_3\text{Ga}_2\text{Ge}_4\text{O}_{14}$, the Ca–O distances are equal to 2.31, 2.51 and 2.68 Å. The last two values correspond to the $g(r)$ minimum of the glass, and there is no correlation between them (see Fig. 4, curve 3). A good agreement between the radial correlations of crystalline and glassy phases was found for the Ga/Ge–O (1.98, 1.87, 1.91 Å) and Ge–O (1.66 Å) distances for the first peak, and for the Ca–Ga (3.33 Å) and Ca–Ge (3.44 Å) for the second peak.

4.4. Molecular dynamic simulations

In Figures 5 and 6, the results of the MD simulation are compared with the X-ray data for $\text{Ca}_3\text{Ga}_2\text{O}_6$ and $\text{Ca}_3\text{Ga}_2\text{Ge}_3\text{O}_{12}$ glasses, respectively. For clearer presentation, only several partial pair distribution functions are shown. As can be seen, our preliminary MD simulation results exhibit a good agreement with the experimental curve.

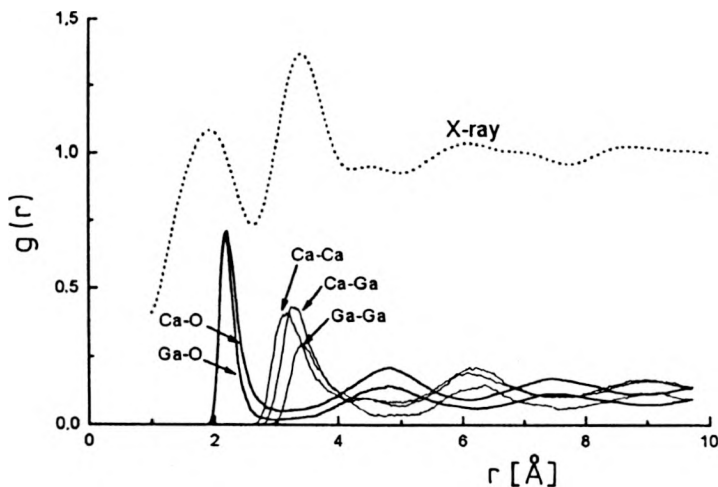


Fig. 5. Pair distribution functions for glasses of $\text{Ca}_3\text{Ga}_2\text{O}_6$ composition: dotted line X-ray scattering method, solid lines – MD simulation, several partial PDFs.

The inspection of the partial pair distribution functions obtained by the MD method leads to the following conclusions.

For $\text{Ca}_3\text{Ga}_2\text{O}_6$ glass, the first diffraction-extracted $g(r)$ peak is formed from the Ca–O and Ga–O contributions. However, the first MD-simulated Ca–O and Ga–O peaks are sharper, and shifted towards larger distances. Distributions of Ca–Ca, Ca–Ga and Ga–Ga distances are responsible for the shape of the second maximum. The third flat experimental peak (at about 4.5 Å) can be related to the second oxygen co-ordination shells around Ca and Ga atoms.

In the case of $\text{Ca}_3\text{Ga}_2\text{Ge}_3\text{O}_{12}$ and $\text{Ca}_3\text{Ga}_2\text{Ge}_4\text{O}_{14}$ glasses, the first diffraction-extracted $g(r)$ peak is mainly related to distribution of Ge–O distances. The MD

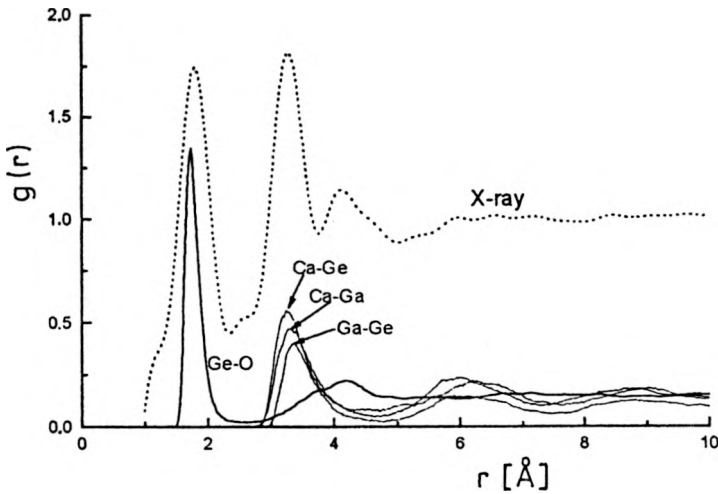


Fig. 6. Pair distribution functions for glasses of $\text{Ca}_3\text{Ga}_2\text{Ge}_3\text{O}_{12}$ composition: dotted line — X-ray scattering method, solid lines — MD simulation, several partial PDFs.

Ca–O and Ga–O partial correlations are placed on the right-hand side of the first experimental maximum, and the most probable Ca–O (2.31 Å) and Ga–O (2.2 Å) distances are rather similar to the corresponding bond lengths in respective crystalline compounds. The second peak of the $g(r)$ function is a sum of pair correlations between Ca, Ga, and Ge atoms, where the Ca–Ge, Ca–Ga, and Ga–Ge pairs give the main contribution. The third peak, which for glasses containing GeO_2 appears for lower r -values, is related mainly to the germanium second oxygen neighbours, and their intensity increases with GeO_2 content.

5. Conclusions

The structure of $\text{Ca}_3\text{Ga}_2\text{Ge}_3\text{O}_{12}$, $\text{Ca}_3\text{Ga}_2\text{Ge}_4\text{O}_{14}$ and $\text{Ca}_3\text{Ga}_2\text{O}_6$ glasses is characterised by the short range chemical ordering, which in its main features is similar to the ordering in the corresponding crystalline compounds. Due to a strong Ge–O correlation, the increase of the GeO_2 content promotes the formation of more and more ordered atomic arrangements. The experimental X-ray data on binary correlation functions remain in a satisfactory agreement with the ones obtained in MD simulations. However, the interaction potential parameters used in the simulations should be much improved, especially for the Ca–O and Ga–O interactions. A more detailed EXAFS study of the $\text{CaO-Ga}_2\text{O}_3\text{-GeO}_2$ compounds is in progress.

Acknowledgments — The authors thank P. Buchynskii from Lviv Scientific and Industrial Amalgamation “Karat” for the synthesis of the glasses. This work has been partly supported by the Gdańsk University, grant No. BW 5200-5-0304-0. The MD simulations have been performed in the TASK Computer Centre in Gdańsk (Poland).

References

- [1] DAMEN J.P.M., PISTORIUS J.A., ROBERTSON J.M., *Mater. Res. Bull.* **12** (1977), 73.
- [2] MILL B.V., BUTASHIN A.V., ELLERN A.M., MAJER A.A., *Izv. Akad. Nauk SSSR, Ser. Neorgan. Mater.* **17** (1981), 1648 (in Russian).
- [3] PADLYAK B.V., BUCHYNSKII P.P., Patent of Ukraine 1998, No. UA 25235 A.
- [4] PADLYAK B.V., LESHCHUK R.YE., MUDRY S.I., *et al.*, [in] Proc. Intern. School—Conference on *Advanced Displays Technologies*, ADTIS '94, [Eds.] J. Stakhira, R. Shuvar, N. Tovstyuk, Lviv State University, Lviv 1994, p. 107.
- [5] PADLYAK B.V., MUDRY S.I., HALCHAK V.P., Abstracts of Intern. Ivan Pulyui Sci. Conference, [Eds.] I. Vakarchuk, Yu. Rudavsky, Lviv State Polytechnical University, Lviv 1995, p. 60.
- [6] MIRKIN L.I., *Handbook on X-Ray Analysis*, Fiz. Mat. Gos. Izd., Moscow 1961 (in Russian).
- [7] NABANA T., MIYAJI T., TAKADA J., *et al.*, *J. Non-Cryst. Solids* **177** (1994), 131.
- [8] ABRAHAMSON A.A., *Phys. Rev.* **178** (1969), 76.
- [9] PRICE D.L., MOSS S.C., REIJERS R., *et al.*, *J. Phys. C* **21** (1988), L1069.

Received September 18, 2000